CRITICAL CONSTANT ILLUMINATION TIME IN COMPARISON OF TWO PHOTOVOLTAIC MAXIMUM POWER POINT TRACKING ALGORITHMS

Ammar AL-GIZI[1,3], Mohamed LOUZAZNI[2], Mustafa Abbas FADEL[3], Aurelian CRACIUNESCU[4]

In this paper, the Perturb and Observe (P&O) and Fuzzy Logic Controlled (FLC) Maximum Power Point Tracking (MPPT) algorithms are analysed in respect with the yield energy of a PV module under different time periods of Standard Technical Conditions (STC). More yield energy can be obtained with P&O MPPT algorithm, for a given duty cycle value of the interfaced DC-DC converter, only in a relative short constant illumination time (CIT). For a relative long CIT, more energy can be obtained with FLC algorithm. The dependence between this CIT and interfaced DC-DC converter's duty cycle (D) is established.

Keywords: Maximum power point tracking, Photovoltaic, Perturb and observe, Fuzzy logic, Duty cycle, Energy yield

1. Introduction

The solar photovoltaic (PV) energy has a nonlinear and explicit characteristic and depends on solar radiation and its distribution, relative humidity, soiling, cable losses, solar cell and ambient temperature that change throughout the day [1-4]. In research literature, there are several models that are focused on the modeling of solar cell and developing several electric models with a different level of complexity; in [5] an available model of solar cell is presented. A mathematical modeling framework to evaluate the performance of single and double diodes has presented in [6,7] presenting details of modelling of a single and double diode to ensure the best suited model under specific environmental condition and effect of various parameters to accurate performance prediction. In [8] it appears using a three-diode model to better explain the current-voltage characteristics of large size industrial silicon solar cells and predicted the

[1] Ph.D. student, Electrical Engineering Faculty, University POLITEHNICA of Bucharest, Romania, e-mail: ammar.ghalib@yahoo.com
[2] Mathematics, Information and Applications Team, National School of Applied Sciences, Abdelmalek Essaadi University, Tanger, Morocco, e-mail: louzazni@msn.com
[3] Faculty of Engineering, Al-Mustansiriyah University, Baghdad, Iraq
[4] Prof., Electrical Engineering Faculty, University POLITEHNICA of Bucharest, Romania, e-mail: aurelian.craciunescu@upb.ro

parameters. In general, there is only one maximum power point (MPP) on PV module curve under uniform and non-uniform solar irradiance condition [9] and change depending on temperature. Therefore, finding the MPP of the PV module is not simple due to the exponential nonlinearity and complexity of the current-voltage equation causes many difficulties. Several papers presented a different method to achieve maximum efficiency for PV systems. Moreover, the used methods and algorithms can be categorized into direct methods or true seeking methods, artificial intelligent methods and indirect methods [10]. The most used methods on direct methods; the hill climbing [11] has been used in perovskite solar cells to investigate the maximum power point tracking (MPPT). The perturbation and observation (P&O) [12-14] or combed with meta-heuristic algorithm [15], and a compared incremental conductance (InC) technique with fuzzy logic (FL) MPP algorithm using modified CUK converter [16]. In [17], the author elaborates a direct and non-iterative MPP finding method for solar PVs based on quadratic regression of the geometry of the power-voltage curve of a typical PV cell or module. A comparative simulation study of MPP algorithms [18] has been presented between P&O, InC, and fuzzy logic controller (FLC) under constant and variable atmospheric conditions. A comparative study of MPP algorithms for PV module BP SX150S has been studied under variable resistive load interfaced to buck-boost converter, at standard technical condition (STC) [19] and variable solar irradiation [20]. The last categories based on the mathematical functions obtained from the empirical current-voltage characteristics to optimize the MPP of PV system [21]. The Newton-raphson method was used in [22] to find the MPP of PV and compared with various classical root-finding methods such as secant method and bisection method.

This paper presents a comparison between two MPPT methods, a classical P&O and FLC methods. Besides, using the commercial PV module BP SX150S [23] will be extracted under STC and interfacing to buck-boost DC-DC converter connected to a MPP algorithm with duty cycle (D) and 6 Ω resistive load. The BP SX150S is a 150 W polycrystalline PV module series provides cost-effective PV power for widespread use, operating DC loads directly or, in an inverter-equipped system, AC loads. The SX 150 is one of the largest products in this series, providing 150 W of nominal maximum power. With 72 cells in series, it charges 24 V batteries or multiples of 24 V efficiently in virtually any climate. It is used primarily in utility grid-supplemental systems, telecommunications, remote villages and clinics, pumping, and land-based aids to navigation. Electrical output is via cables terminated with installation-speeding polarized connectors. The energy yield at the output of PB SX150S PV module versus time will be controlled and compared using the variable ΔD of the symmetrical FLC and fixed for P&O MPPT algorithms to function in maximum power. Meanwhile, the FLC of one input, $\Delta P/\Delta V$ and one output, ΔD, is used. Moreover, the P&O of different

values of ΔD during each time period is also presented. The obtained results represent the effect of fixed and variable ΔD on the energy yield of commercial PV module. The useful comparison between FLC and P&O MPPT algorithms for the PV module by which it makes it convenient to choose the efficient algorithm for solar PV systems during any period of time.

2. Maximum power point tracking techniques

In the recent paper, the determination of maximum power tracking is mandatory for PV power system. The characteristics of a PV system that determines the operating points are the power-voltage curve and current-voltage curve [24]. Further, the maximum power is extracted while operating at the intersection of the *I-V* and *P-V* curve namely maximum current I_{mpp} and voltage V_{mpp} as shows in Fig .1.

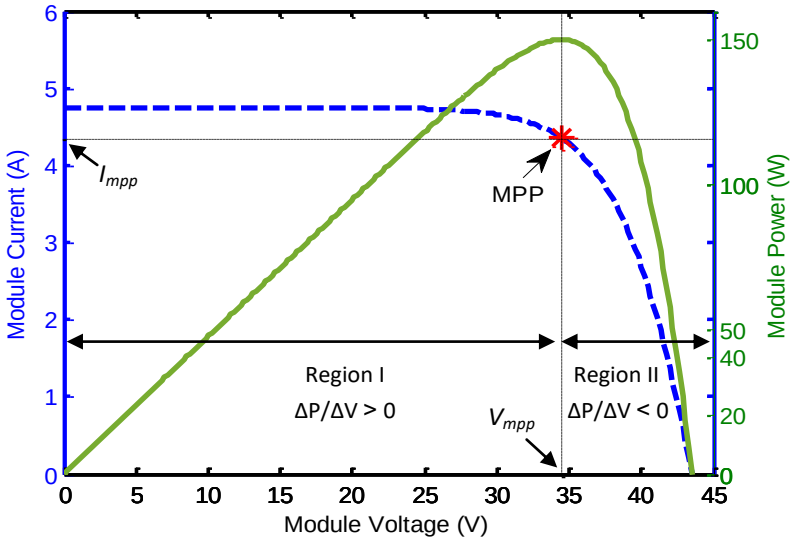

Fig. 1. *I-V* and *P-V* characteristics of a BP SX 15S PV module at STC

Several papers have used the commercial PV module BP SX150S for searching the MPP. Further, the FLC is used in [26] with adaptive output scaling factor as a MPPT of PV system, and in [27] using with genetic algorithm and FPGA. Other papers have extracted the maximum power point of BP SX150S presenting the comparative study using different DC-DC converter with standalone PV system [20] and based in power electronic transformer [28]. Moreover, our work will be based in the FLC and P&O techniques as a hybrid control between artificial and conventional MPPT algorithms to compare and extract the maximum power from the BP SX150S PV module connected.

A typical functional diagram of a PV energy conversion system is depicted in Fig. 2.

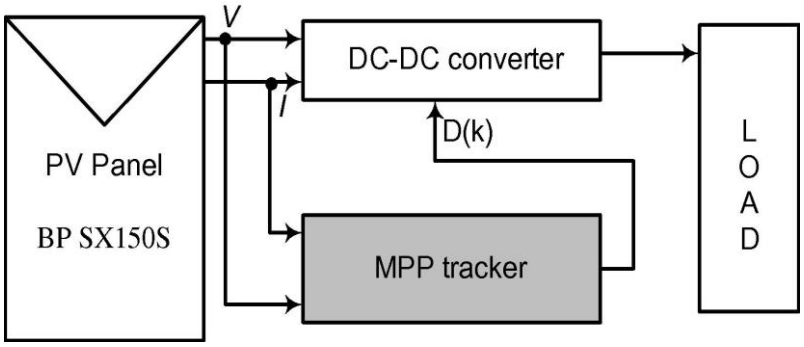

Fig. 2. The photovoltaic system with MPPT

The system consists of a commercial BP SX150S PV module of 72 solar cells connected in series. It can charge 24 V batteries or multiples of 24 V efficiently in virtually any climate and it is capable of producing a maximum power of 150 W under STC, interfaced to buck-boost DC-DC converter connected to a MPP algorithm with duty cycle and 6 Ω of resistive load. The MPPT has the objective to draw as much power as possible from PV module under all operating conditions by adjusting continuously the duty cycle of the DC-DC converter.

The electrical parameters of BP SX150S at STC are summarized in Table 1 [25]

Table 1

Electrical parameters of BP SX150S PV module at STC

Parameter	Value
Maximum power (P_{max})	150 W
Voltage at P_{max} (V_{mpp})	34.5 V
Current at P_{max} (I_{mpp})	4.35 A
Warranted minimum P_{max}	140 W
Short-circuit current (I_{sc})	4.75 A
Open-circuit voltage (V_{oc})	43.5 V
Maximum system voltage	600 V
Temperature coefficient of I_{sc}	(0.065 ± 0.015) %/ ^{o}C
Temperature coefficient of V_{oc}	(160 ± 20) mV/ ^{o}C
Temperature coefficient of power	(0.5 ± 0.05) %/ ^{o}C
NOCT	47 ± 2 ^{o}C

Fig. 3 shows the basic circuit of buck-boost DC-DC converter used in the analyzed PV system. The power switch S_W modulates the energy transfer from the input source to the load when controlled by a varying *D*.

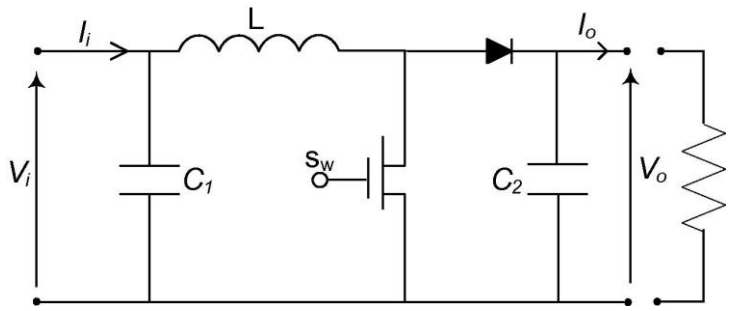

Fig. 3. Basic circuit of the buck-boost DC-DC converter

The continuous current average model of the buck-boost converter is governed by the following basic equations:

$$\begin{cases} V_o = \dfrac{D}{1-D} \times V_i \\ I_i = \dfrac{D}{1-D} \times I_o \end{cases}, \tag{1}$$

where, V_i and I_i are respectively the voltage and current at the input point, V_o and I_o are respectively the voltage and current at the output point.

The main purpose of the DC-DC converter is the maintaining of the matching between the input impedance of the converter R_{in} and the PV optimal impedance R_{opt} for locating the operating point at MPP, thereby extracting a maximum available power from the PV module. R_{opt} can be represented by:

$$R_{opt} = \frac{V_{mpp}}{I_{mpp}}, \tag{2}$$

where, V_{mpp} and I_{mpp} are voltage and current of PV module at the MPP, respectively. Based on the utilized ideal DC-DC converter, the relationship between R_{in}, load impedance R_{Load}, and duty cycle (D) can be described by:

$$R_{in} = \frac{V}{I} = \frac{(1-D)^2}{D^2} \times \frac{V_{Load}}{I_{Load}} = \frac{(1-D)^2}{D^2} \times R_{Load}, \tag{3}$$

where, V and I are the voltage and current of PV panel. Whereas, V_{Load} and I_{Load} are voltage and current of the load, respectively.

By controlling the value of D, the R_{opt} can be maintained. Hence, by increasing D, R_{in} will be decreased and the operating point will be moved in anti-clockwise direction and vice versa.

Fig. 4 shows the relationship between duty cycle and the delivered power from photovoltaic panel at various values of R_{Load} at STC. It can be seen from Fig. 4 that the optimal D for different value of load resistance increases to reach the unique MPP when the load resistance increased.

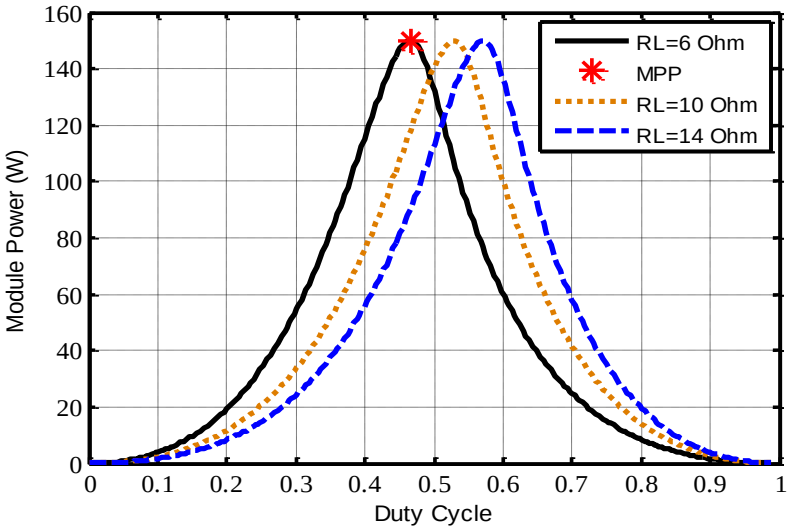

Fig. 4. Module power vs duty cycle under variable resistive load at STC

3. Perturb and observe (P&O) algorithm

For the low cost, simple implementation, little maintenance and supervision, the conventional P&O MPPT algorithm is generally preferred. Furthermore, the method is based on their reference perturbation parameter as voltage perturbation, current perturbation and direct duty ratio perturbation. Moreover, the power (P) is computed using the measured values of the voltage (V) and current (I) of the photovoltaic array. The algorithm provides a perturbation (ΔV) in V, based on the change of P by the following rules:

$$\begin{cases} V_{new} = V_{old} + \Delta V \times slope & if \;\; P > P_{old} \\ V_{new} = V_{old} - \Delta V \times slope & if \;\; P < P_{old} \end{cases}, \tag{4}$$

The slope in (4) indicates the direction of the perturbation, i.e. to the right (climbing) or left (descending), as shown in Fig. 5.a. The size of the perturbation ΔV is crucial if ΔV is large and the convergence is fast, but it results in large fluctuation in P, and vice versa. Algorithm will cause the operating point to continuously oscillate around the MPP, as depicted in Fig. 5.b. Obviously the loss is more, if the perturbation size is large. The oscillation is highly undesirable as it results is significant energy loss.

The P&O algorithm starts by settling the computed P_{max} to initial value. Next the actual PV voltage and current are measured at specific interval and P_{act} is calculated. P_{max} and P_{act} are compared.

The flow chart of P&O MPPT algorithm is depicted in the Fig. 6.

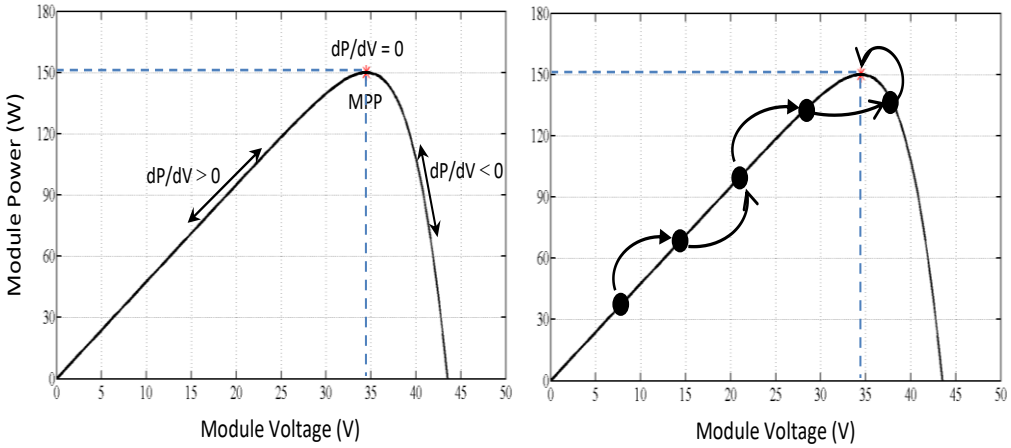

Fig. 5. (a) Operating point according to the sign of dP/dV; (b) MPPT using P&O algorithm

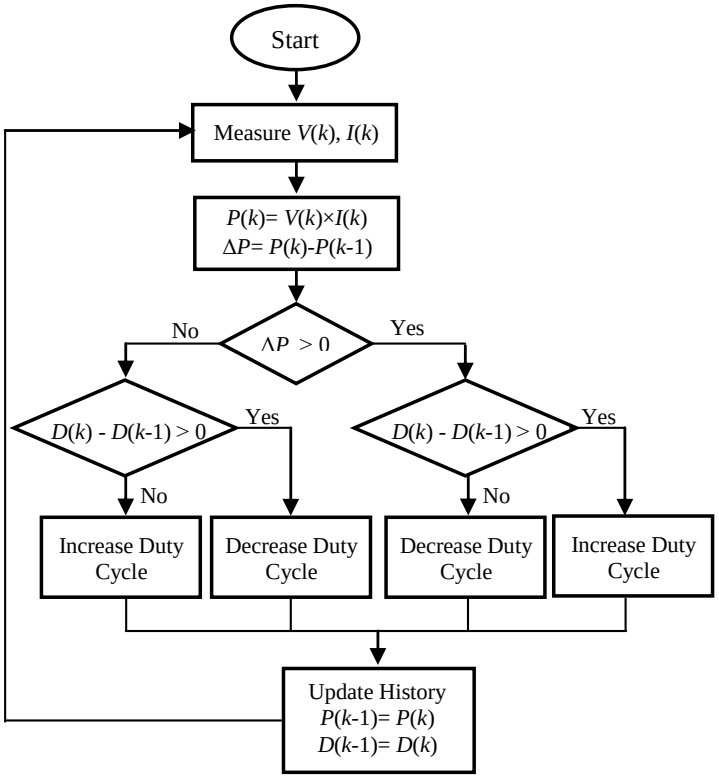

Fig. 6. Flow chart of P&O algorithm

4. Fuzzy logic controller (FLC)

Generally, fuzzy logic control is used to convert a complex system to a list of rules and solving without needing to use a mathematical model. Additionally, the fuzzy logic is used to adjust the duty cycle (*D*) of DC-DC converter to maintain the MPPT. The fuzzy logic MPPT doesn't need the knowledge about model of the photovoltaic system. The basic structure of fuzzy logic based MPPT controller is shown in Fig. 7.

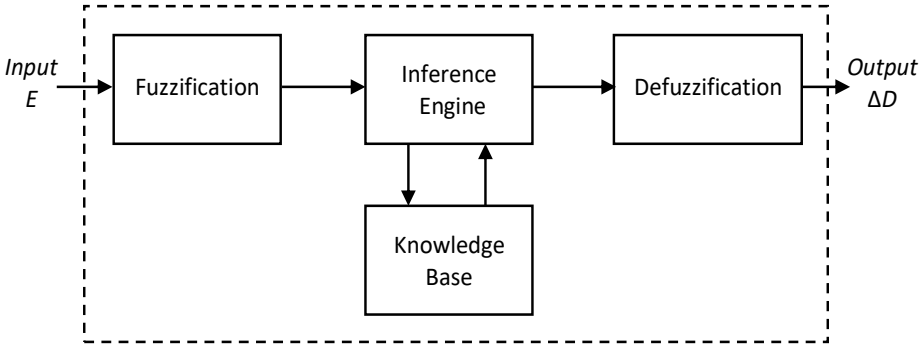

Fig. 7. Structure of the fuzzy logic controller

In this work, a single input and output variables are used for the FLC: The first input is $E(k)$, and output control signal is the change in the duty cycle $\Delta D(k)$. The inputs and output, at a sampling instant *k* are expressed as follows:

$$E(k) = \frac{P(k) - P(k-1)}{V(k) - V(k-1)}; \tag{5}$$

$$D(k) = D(k-1) + \Delta D(k). \tag{6}$$

Where, $P(k)$ and $V(k)$ are the output power and voltage of the PV module at sampling *k*. $P(k-1)$ and $V(k-1)$ are the previous power and voltage of PV panels. $\Delta D(k)$ is the change in duty ratio used as the FLC's variable control output to calculate the DC-DC converter's actual duty ratio $D(k)$ at sampling *k*. While $E(k)$ is the *P*-*V* curve's slope. Consequently, the sign of $E(k)$ shows the operating point's location at instant *k*, either on the left or on the right of MPP on the *P*-*V* curve of PV module, as illustrated in Fig. 8.

When change in $P(k) - P(k-1) > 0$ and $V(k) - V(k-1) > 0$ are positive, to reach the MPPT, the voltage should be increased. That is illustrated with red arrow in Fig. 8. When change in power $P(k) - P(k-1) > 0$ is positive and change in voltage $V(k) - V(k-1) < 0$ is negative, to reach the MPPT, the voltage should be

decreased. That is illustrated with purple arrow in Fig. 8. When change in power $P(k)-P(k-1)<0$ is negative and change in voltage $V(k)-V(k-1)>0$ is positive, to reach the MPP, the voltage should be decreased. That is illustrated with green arrow in Fig. 8. When change in power $P(k)-P(k-1)<0$ and voltage $V(k)-V(k-1)<0$ are negative, to reach the MPPT, the voltage should be increased, that is illustrated with blue arrow in Fig. 8 [29-31]. Furthermore, it can be seen from Fig. 8, that the positive *P-V* slope at left side is smaller than the negative slope at the right side of the curve.

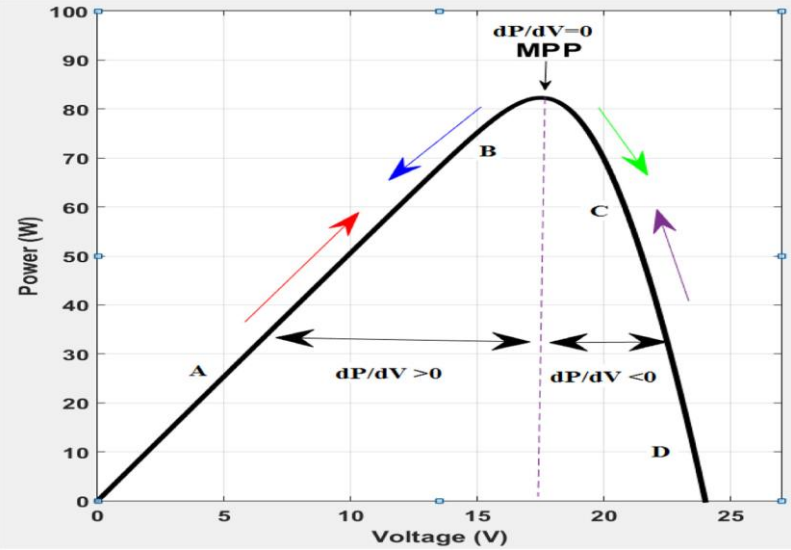

Fig. 8. P-V characteristic of PV panel for MPPT algorithm

The next step is creating rule table and membership functions for Fuzzy logic. The rule base (RB) table of FLC MPPT is shown in Table 2, and the membership functions (MFs) are shown in Fig. 9. Several types and numbers of MFs can be used in the design of FLC [31].

In this paper, a symmetrical FLC of five triangular MFs is used. Where, those MFs are labelled with a linguistic term: negative big (NB), negative small (NS), zero (Z), positive small (PS), and positive big (PB). In contrast, the minimum and maximum limits of $\Delta P/\Delta V$ are set as -43.5 and 43.5, respectively. However, the limits of ΔD are set as -0.05 and 0.05, respectively [32].

Table 2

Rule-Base of the symmetrical FLC of five MFs

$\Delta P/\Delta V$	NB	NS	Z	PS	PB
ΔD	PB	PS	Z	NS	NB

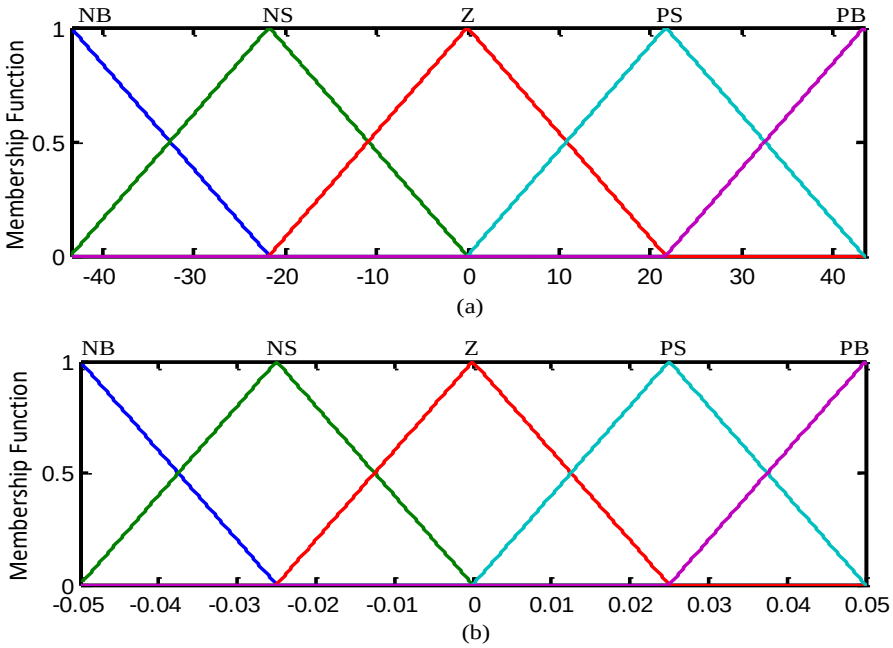

Fig. 9. Membership functions of the symmetrical FLC: (a) Input $\Delta P/\Delta V$; (b) Output ΔD

5. Simulation results and discussion

To evaluate the solar energy yield from a PV system using P&O and FLC MPPT algorithms, a commercial PV module BP SX150S of parameters showed in Table 1 is used. The PV module is interfaced to a 6 Ω resistive load, through an ideal buck-boost DC-DC converter driven by a MPPT algorithm used to generate a proper control duty cycle (D).

The extractable power from the PV module and the corresponding solar energy using MPPT algorithms are illustrated in Fig. 10 and Fig. 11, respectively. The power output and energy yield based on P&O MPPT algorithms is evaluated at different values of ΔD and under STC during 60 s of time.

The formula of energy yield used in the simulation, can be expressed by:

$$Energy\,Yield\,(Wh) = \frac{\int_0^{t_f} P(t)\,dt}{3600}, \tag{7}$$

where, P(t) is the module power at time t, and t_f is the final time.

By increasing ΔD, the tracking speed of P&O algorithm is increased with an increasing in the power oscillation around MPP. However, the FLC MPPT algorithm can reach the MPP with less oscillation, as shown in Fig. 10. Hence, the FLC MPPT algorithm can harvest more energy yield than the P&O algorithm, as

shown in Fig. 11. The following Fig. 12, 13 and 14 show the increasing effect of ΔD on the energy yield from PV module using the proposed MPPT algorithms. Those figures show the effect at different time periods of 10.72 s, 32.14 s, and 48.24 s, respectively. In spite of the large power oscillation around MPP; at 48.24 s, the P&O can harvest more energy than FLC for $0.0076 \leq \Delta D \leq 0.045$, due to the small rising time compared with the FLC algorithm. While this amelioration of the P&O, is significantly decreased for $\Delta D > 0.045$, due to the increasing in its power oscillation around MPP. Knowing that the ideal and actual energy yield (using FLC) is 2.01 Wh and 1.82 Wh, respectively, as shown in Fig. 12. Fig. 13 and Fig. 14 show that the optimum range of ΔD at which the P&O can harvest more energy than FLC is significantly increased by decreasing time. Where, the ranges are $0.0075 \leq \Delta D \leq 0.06$ and $0.0073 \leq \Delta D \leq 0.165$ at time periods of 32.14 s and 10.72 s, respectively. Besides, the actual energy yield using FLC is 1.15 Wh and 0.255 Wh, at time periods of 32.14 s and 10.72 s, respectively. In contrast, the ideal energy yields at these periods are 1.337 Wh and 0.446 Wh, respectively.

Moreover, according to a different time periods, Fig. 15 reveals the required optimum value of ΔD for P&O algorithm to satisfy the energy yield intersection point with the FLC MPPT algorithm.

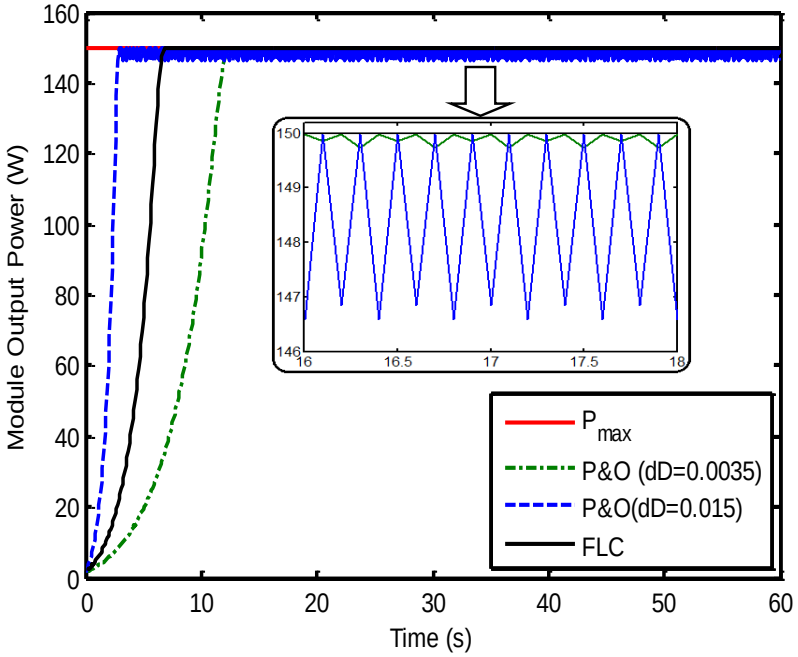

Fig. 10. Output power using MPPT methods under STC and different values of ΔD

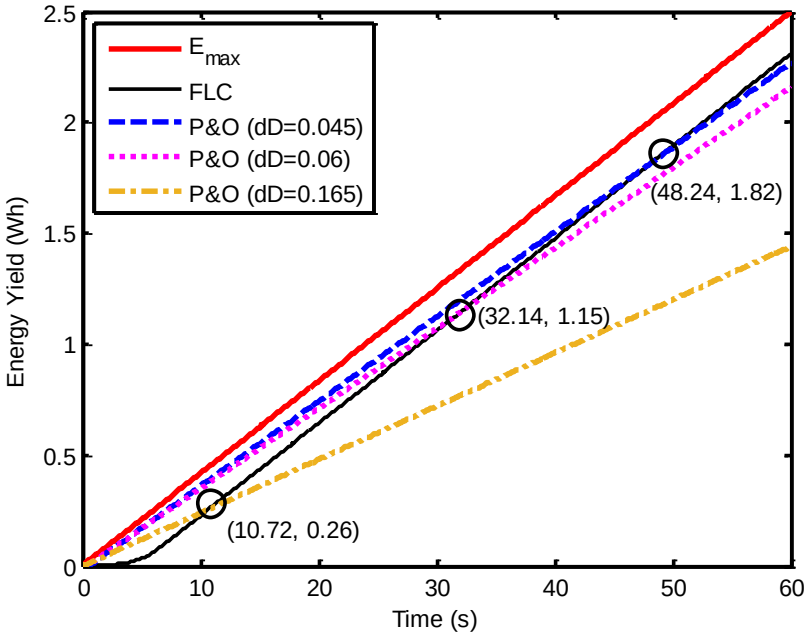

Fig. 11. Energy yield using MPPT methods under STC and different values of ΔD

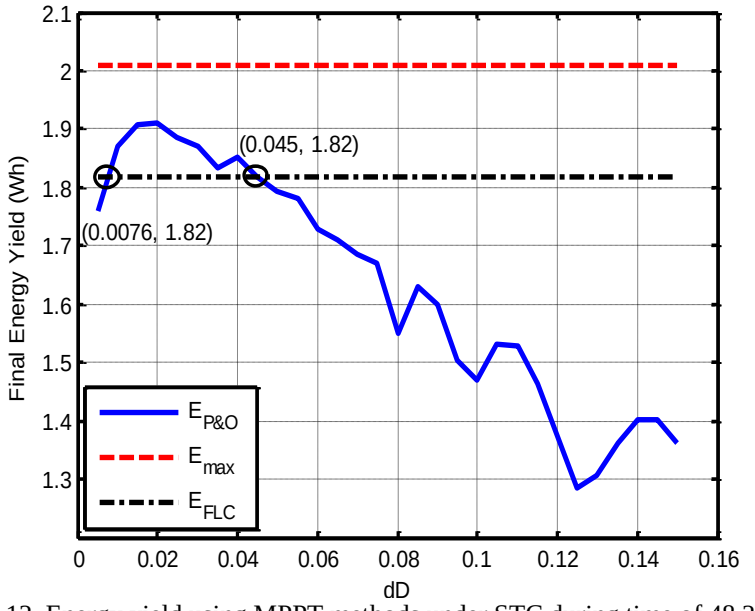

Fig. 12. Energy yield using MPPT methods under STC during time of 48.24 s

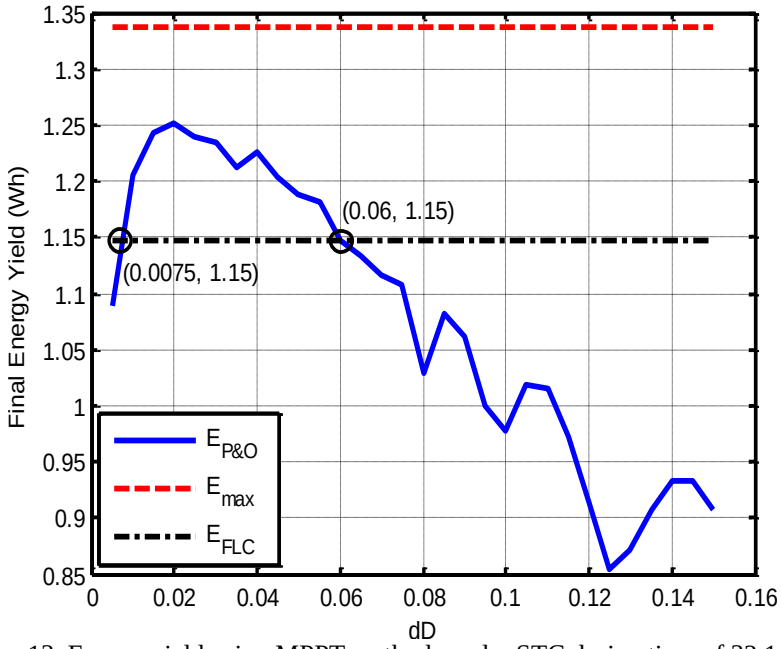

Fig. 13. Energy yield using MPPT methods under STC during time of 32.14 s

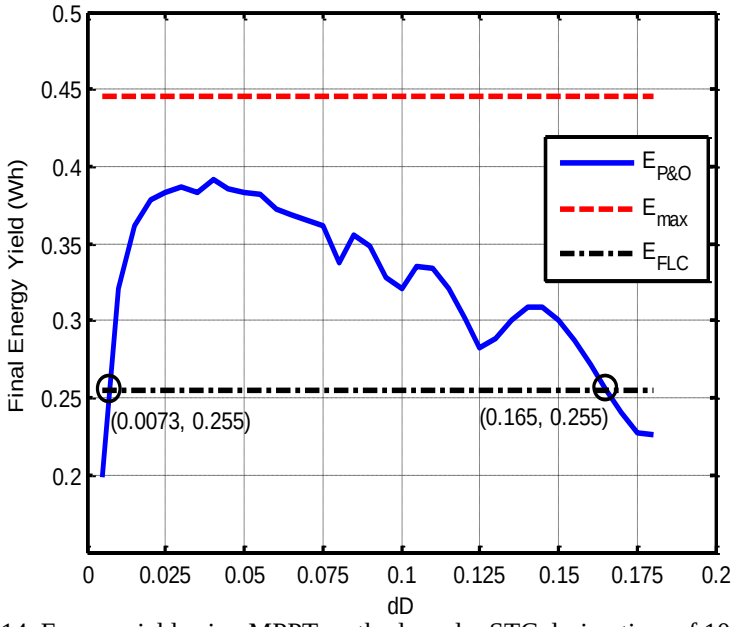

Fig. 14. Energy yield using MPPT methods under STC during time of 10.72 s

It is evident from Fig. 15 that by decreasing the time, the ΔD required for the energy yield intersection between P&O and FLC will be significantly increased, due to the decreasing in rising time and increasing in the oscillation

around MPP for the P&O algorithm. For time periods of 48.24 s, 32.14 s, and 10.72 s, the corresponding Δ*D* required for the intersection points A, B, and C are 0.045, 0.06, and 0.165, respectively, as shown in Fig. 15.

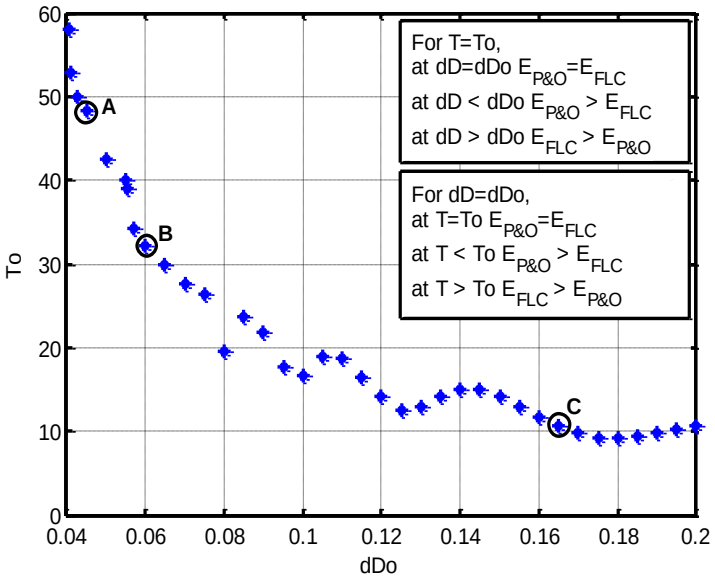

Fig. 15. Energy yield intersection points between FLC and P&O MPPT algorithms under STC

6. Conclusions

This paper presents the possibility of increasing the energy yield of PV system based on P&O MPPT algorithm under STC, during different periods of time.

Although the MPPT speed based on P&O algorithm is significantly increased by increasing Δ*D*, the power oscillation around the MPP is also increased, resulting an increasing in the power loss at the steady state, as shown in Fig. 10. Hence the energy yield based on the P&O algorithm can be increased and intersects with that obtained by the FLC algorithm by increasing Δ*D*, at a specific time of STC, as shown in Fig. 11. Moreover, P&O MPPT algorithm can produce more energy yield than that of FLC algorithm at the specific range of Δ*D* corresponding to the time period of STC, as shown in Fig. 12, Fig. 13, and Fig. 14. The intersection point and optimum range of Δ*D* are significantly increased by increasing the frequency of irradiation under STC, as shown in Fig. 15. Consequently, the careful selection of ΔD for P&O MPPT algorithm plays an important role in improving the performance of the PV system, thus harvesting more solar energy yield in comparison with the FLC MPPT algorithm.

R E F E R E N C E S

[1]. *M. Louzazni, A. Khouya, K. Amechnoue, A. Crăciunescu and M. Mussetta*, Comparative prediction of single and double diode parameters for solar cell models with firefly algorithm, in 2017 10th International Symposium on Advanced Topics in Electrical Engineering (ATEE), 2017, pp. 860-865.

[2]. *A. G. Al-Gizi, A. Craciunescu and S. J. Al-Chlaihawi*, The use of ANN to supervise the PV MPPT based on FLC, in 2017 10th International Symposium on Advanced Topics in Electrical Engineering (ATEE), 2017, pp. 703-708.

[3]. *T. Minemoto, S. Nagae and H. Takakura*, Impact of spectral irradiance distribution and temperature on the outdoor performance of amorphous Si photovoltaic modules, Sol. Energy Mater. Sol. Cells, **vol. 91**, no 10, Jun. 2007, pp. 919-923.

[4]. *E. Elibol, Ö. T. Özmen, N. Tutkun and O. Köysal*, Outdoor performance analysis of different PV panel types, Renew. Sustain. Energy Rev., **vol. 67**, Jan. 2017, pp. 651-661.

[5]. *M. A. Hasan and S. K. Parida*, An overview of solar photovoltaic panel modeling based on analytical and experimental viewpoint, Renew. Sustain. Energy Rev., **vol. 60**, Jul. 2016, pp. 75-83.

[6]. *S. Bana and R. P. Saini*, A mathematical modeling framework to evaluate the performance of single diode and double diode based SPV systems, Energy Rep., **vol. 2**, 2016, pp. 171-187.

[7]. *M. H. El-Ahmar, A. H. M. El-Sayed and A. M. Hemeida*, Mathematical modeling of photovoltaic module and evaluate the effect of various parameters on its performance, in 2016 Eighteenth International Middle East Power Systems Conference (MEPCON), 2016, pp. 741-746.

[8]. *V. Khanna, B. K. Das, D. Bisht, Vandana and P. K. Singh*, A three diode model for industrial solar cells and estimation of solar cell parameters using PSO algorithm, Renew. Energy, **vol. 78**, Jun. 2015, pp. 105-113.

[9]. *E. Kandemir, N. S. Cetin and S. Borekci*, A comprehensive overview of maximum power extraction methods for PV systems, Renew. Sustain. Energy Rev., **vol. 78**, Oct. 2017, pp. 93-112.

[10]. *D. Verma, S. Nema, A. M. Shandilya and S. K. Dash*, Maximum power point tracking (MPPT) techniques: Recapitulation in solar photovoltaic systems, Renew. Sustain. Energy Rev., **vol. 54**, Feb. 2016, pp. 1018-1034.

[11]. *N. Pellet et al.*, Hill climbing hysteresis of perovskite-based solar cells: a maximum power point tracking investigation, Prog. Photovolt. Res. Appl., pp. n/a-n/a.

[12]. *R. Faranda, S. Leva and V. Mauger*, Comparative study of ten maximum power point tracking algorithms for photovoltaic system, U. P. B. Sci. Bull., Series C, **vol. 69**, no. 4, 2007 ISSN 1454-234x.

[13]. *M. L. Florea and A. Baltatanu*, Modeling and testing of maximum power point tracking algorithms for photovoltaic systems, U. P. B. Sci. Bull., Series C, **vol. 77**, no. 4, 2015, pp. 373-382.

[14]. *M. Prasad and A. K. Akella*, Comparative analysis of solar photovoltaic fed Z-source inverter based UPQC for power quality enhancement, U. P. B. Sci. Bull., Series C, **vol. 79**, no. 3, 2017, pp. 123-140.

[15]. *S. Mohanty, B. Subudhi and P. K. Ray*, A Grey Wolf-assisted perturb observe MPPT algorithm for a PV System, IEEE Trans. Energy Convers., **vol. 32**, no 1, March 2017, pp. 340-347.

[16]. *A. M. Farayola, A. N. Hasan and A. Ali*, Comparison of modified incremental conductance and fuzzy logic MPPT algorithm using modified CUK converter, in 2017 8th International Renewable Energy Congress (IREC), 2017, pp. 1-6.

[17]. *G. Kumar, M. B. Trivedi and A. K. Panchal*, Innovative and precise MPP estimation using P–V curve geometry for photovoltaics, Appl. Energy, **vol. 138**, Jan. 2015, pp. 640-647.
[18]. *A. G. Al-Gizi and S. J. Al-Chlaihawi*, Study of FLC based MPPT in comparison with P&O and InC for PV systems, in 2016 International Symposium on Fundamentals of Electrical Engineering (ISFEE), 2016, pp. 1-6.
[19]. *A. G. Al-Gizi*, Comparative study of MPPT algorithms under variable resistive load, in 2016 International Conference on Applied and Theoretical Electricity (ICATE), 2016, pp. 1-6.
[20]. *A. Al-Gizi, S. Al-Chlaihawi and A. Craciunescu*, Efficiency of photovoltaic maximum power point tracking controller based on a fuzzy logic, Advances in Science, Technology and Engineering Systems Journal (ASTES), **vol. 2**, no. 3, 2017, pp. 1245-1251.
[21]. *V. Salas, E. Olías, A. Barrado and A. Lázaro*, Review of the maximum power point tracking algorithms for stand-alone photovoltaic systems, Sol. Energy Mater. Sol. Cells, **vol. 90**, no 11, Jul. 2006, pp. 1555-1578.
[22]. *S. Chun and A. Kwasinski*, Analysis of classical root-finding methods applied to digital maximum power point tracking for sustainable photovoltaic energy generation, IEEE Trans. Power Electron., **vol. 26**, no. 12, Dec. 2011, pp. 3730-3743.
[23]. http://www.abcsolar.com/pdf/bpsx150.pdf
[24]. *P. Vinay and M. A. Mathews*, Modelling and analysis of artificial intelligence based MPPT techniques for PV applications, in 2014 International Conference on Advances in Green Energy (ICAGE), 2014, pp. 56-65.
[25]. *A. Al-Gizi, A. Craciunescu and S. Al-Chlaihawi*, Improving the performance of PV system using genetically-tuned FLC based MPPT, in 2017 International Conference on Optimization of Electrical and Electronic Equipment (OPTIM) 2017 Intl Aegean Conference on Electrical Machines and Power Electronics (ACEMP), 2017, pp. 642-647.
[26]. *O. Guenounou, B. Dahhou and F. Chabour*, Adaptive fuzzy controller based MPPT for photovoltaic systems, Energy Convers. Manag., **vol. 78**, no. Supplement C, Feb. 2014, pp. 843-850.
[27]. *A. Messai, A. Mellit, A. Guessoum and S. A. Kalogirou*, Maximum power point tracking using a GA optimized fuzzy logic controller and its FPGA implementation, Sol. Energy, **vol. 85**, no. 2, Feb. 2011, pp. 265-277.
[28]. *M. Razmkhah, M. R. Azizian and H. M. Kojabadi*, Photovoltaic systems based on power electronic transformer with maximum power tracking capability, in 2017 Conference on Electrical Power Distribution Networks Conference (EPDC), 2017, pp. 74-79.
[29]. *U. Yilmaz, A. Kircay and S. Borekci*, PV system fuzzy logic MPPT method and PI control as a charge controller, Renew. Sustain. Energy Rev., **vol. 81**, no. 1, Jan. 2018, pp. 994-1001.
[30]. *A. Al Nabulsi and R. Dhaouadi*, Efficiency optimization of a DSP-based standalone PV system using fuzzy logic and dual-MPPT control, IEEE Trans. Ind. Inform., **vol. 8**, no. 3, Aug. 2012, pp. 573-584.
[31]. *A. Al-Gizi, S. Al-Chlaihawi, M. Louzazni and A. Craciunescu*, Genetically optimization of an asymmetrical fuzzy logic based photovoltaic maximum power point tracking controller, Advances in Electrical and Computer Engineering, **vol. 17**, no. 4, 2017, pp. 69-76.
[32]. *A. Al-Gizi, S. Al-Chlaihawi, A. Craciunescu*, Comparative study of some FLC-based MPPT methods for photovoltaic systems, MATTER: International Journal of Science and Technology, **vol. 3**, no. 3, 2017, pp. 36-50.